ELSEVIER

Catalysis Today 55 (2000) 291–299

CATALYSIS TODAY

www.elsevier.com/locate/cattod

In situ infrared study of catalytic decomposition of NO on carbon-supported Rh and Pd catalysts

K. Almusaiteer, R. Krishnamurthy, S.S.C. Chuang *

Department of Chemical Engineering, The University of Akron, Akron, OH 44325–3906, USA

Abstract

The direct catalytic decomposition of NO on Rh/Al_2O_3, Rh/C, Pd/Al_2O_3, and Pd/C catalysts was investigated at 673 K by in situ infrared (IR) coupled with mass spectroscopy (MS). NO decomposition on these catalysts initially produced N_2 and adsorbed oxygen. Different catalysts exhibit different capabilities for manipulating adsorbed oxygen. Rh/Al_2O_3 shows little activity for oxygen desorption, resulting in loss of catalyst activity; Rh/C shows the ability for promoting the adsorbed oxygen–carbon reaction, removing oxygen in the form of CO_2; Pd/Al_2O_3 shows some activity for O_2 desorption. Use of carbon as a support for Pd promotes O_2 desorption, resulting in improvement of NO decomposition activity. The in situ IR results provide evidence to support the behavior of adsorbed oxygen on carbon-supported Rh and Pd catalysts.

Keywords: Infrared spectroscopy; NO decomposition; Oxygen desorption; Rh; Pd; Activated carbon; Adsorption; Adsorbed NO

1. Introduction

NO is a major pollutant in the exhaust of various combustion processes. The growing concerns for the environment have resulted in increasingly stringent NO emission standards [1–3]. Removal of NO from the exhaust streams of automobiles, power plants, and other combustion processes has become a challenging task.

Depending on the nature of the combustion process, various approaches for NO removal have been developed. The catalytic approaches for the removal of NO include:

1. the reaction of NO with CO [1–4];
2. selective catalytic reduction with NH_3 and hydrocarbons [5,6]; and
3. the direct decomposition of nitric oxide [7–10].

The advantages and disadvantages of each approach are listed in Table 1.

The direct decomposition of NO, $2NO \rightarrow N_2 + O_2$, is the most attractive approach for NO removal, because of its simplicity [7]. It is thermodynamically favorable at temperatures <2000 K. For the NO decomposition catalyst development, the two critical issues to be addressed are catalyst activity and durability [11].

Studies on the proposed elementary steps for NO decomposition have revealed that the low activity of the catalysts is due to their inability to desorb oxygen produced from NO dissociation [8,10]. Oxygen from dissociated NO is strongly bonded to the catalyst surface, poisoning NO dissociation sites and inhibiting further NO dissociation. Various approaches to remove adsorbed oxygen from the NO dissociation sites include:

1. thermal desorption;
2. autoreduction of the surface in He flow [8]; and
3. spillover of adsorbed oxygen [10].

* Corresponding author. Tel.: +1-330-972-6993; fax: +1-330-972-5856.

0920-5861/00/$ – see front matter
PII: S0920-5861(99)00242-4

Table 1
Advantages and disadvantages of individual approaches

Approach	Disadvantages	Advantages
Catalytic reduction of NO with CO over three-way catalysts (Pt–Rh or Pd)	ineffective under net oxidizing conditions sulfur poisoning high Pt and Rh metal costs	simultaneous removal of CO, NO and hydrocarbons
Selective catalytic reduction with NH_3	special handling and storage of NH_3 special metering system to avoid NH_3 slippage very high capital costs	high NO removal efficiency in the presence of O_2.
Selective catalytic reduction with hydrocarbons	further improvement in the selectivity to N_2 is needed. Hydrocarbon slippage.	potential for high NO removal efficiency in the presence of O_2
Direct decomposition of NO		chemical simplicity to form N_2 and O_2.
perovskite type catalysts	low activity and conversions	eliminating the use of reducing agents
Cu-ZSM-5	a narrow temperature window of operation and susceptible to water and SO_2 poisoning	
Pt/Al_2O_3 based catalysts	low activity due to inability to desorb oxygen	
Tb- promoted catalysts	loss of catalyst activity in the presence of O_2.	

One possible approach is to use carbon as a support for the catalyst system, facilitating the removal of oxygen by the formation of CO_2. Recent studies have shown that activated carbon has the capability to reduce NO to form N_2 and CO_2 [12–14]. Near 100% conversions of NO were achieved using an Ni or Co catalyst supported on activated carbon at temperatures >713 K. The NO conversions on carbon-supported catalysts decreased in the presence of O_2 [15].

Rhodium (Rh) and Palladium (Pd), the major components in three way catalytic converters, have shown excellent activity for the dissociation of adsorbed NO. To determine the feasibility of using carbon for removal of adsorbed oxygen on Rh and Pd, we have examined the activity of carbon- and Al_2O_3-supported Rh and Pd catalysts, and the nature of the adsorbate for the NO decomposition reaction. We have found that carbon promotes the N_2 and CO_2 formation over Rh catalyst while enhancing N_2 and O_2 formation on Pd catalyst.

2. Experimental

The 2 wt.% Rh/Al_2O_3, 2 wt.% Rh/C, 2 wt.% Pd/Al_2O_3, and 2 wt.% Pd/C catalysts were prepared by incipient wetness impregnation technique of large surface area γ-Al_2O_3 (Alfa Products, 100 m^2/g surface area) and carbon (activated carbon, Ambersorb 563, Rohm & Haas, 550 m^2/g surface area) with $RhCl_3$ or $PdCl_2$ solutions. The ratio of the volume of the solution to the weight of the support used in the impregnation step was 1 cm^3 : 1 g. The catalysts were dried overnight in air at 303 K. They were then calcined in air at 673 K for 8 h and reduced in flowing H_2 at 673 K for 8 h. The crystallite size of Rh and Pd was characterized by X-ray diffraction (XRD). The crystallite sizes of Rh in Rh/Al_2O_3 and Pd in Pd/Al_2O_3 were found to be 50 and 64 Å, respectively. The crystallite sizes of Rh in Rh/C and Pd in Pd/C were found to be 47 and 70 Å, respectively.

Al_2O_3-supported catalysts were pressed in the form of self-supporting disks (40 mg each); one of the disks was placed in the infrared (IR) cell for in situ transmission IR studies and the other two disks were broken down into flakes and placed in the exit line of the IR reactor cell [16]. The additional catalyst disks were used to increase the amount of desorbing species and conversions to obtain a strong signal in the mass spectrometer (MS). Carbon-supported catalysts were diluted with KBr (catalyst: KBr = 1 : 10), and 20 mg of the solid mixture were placed in the diffuse-reflectance infrared Fourier transform (DRIFT) cell in a powder form for in situ IR studies.

Additional carbon-supported catalyst (90 mg) was placed in a tubular reactor, which was connected in series with the DRIFT cell.

The catalysts were reduced in situ in flowing H_2 at 673 K for 1 h. Following the in situ reduction of the catalyst, the NO decomposition study was carried out at 673 K. The catalyst was exposed initially to He flow. A 4-port valve was used to switch the He flow to 1% NO in He flow in a step mode. This NO step switch technique allows investigating the sequence of adsorbate and product formation during the NO decomposition reaction on the catalyst surface. Fourier transform infrared spectroscopy (FTIR) was used to monitor the adsorbate concentrations and MS to analyze the change in the concentration of the gaseous product from the effluent of the IR reactor cell.

3. Results

3.1. NO decomposition on Rh/Al_2O_3

Fig. 1(a) shows the MS analysis of the IR reactor cell effluent during the 1% NO step switch reaction studies on Rh/Al_2O_3 at 673 K. The IR spectra of the adsorbates corresponding to the MS profiles are shown in Fig. 2. To determine the role of adsorbates in the reaction, the variation in the IR intensity of major adsorbates was plotted vs. time in Fig. 1b. Absence of adsorbed species prior to the step switch indicates that the catalyst surface was clean. The step switch from He to 1% NO at $t = 0$ resulted in the formation of N_2. The absence of NO in the initial period is a result of near 100% conversion. Ar, the species added in 1% NO flow, shows that a near-perfect step switch was achieved. A close examination of MS and IR intensity profiles in Fig. 1(a) and (b) revealed that the NO step switch reaction may be divided into three stages. Stage 1 comprises nearly complete NO conversions on the reduced metal surface, resulting in the depletion of all the NO adsorbates in the 0–10 min period; Stage 2 is the emergence of NO adsorbates in the 10–31 min period; and Stage 3 is the appearance and slow growth of gaseous NO profile after 31 min. The wavering behavior of the MS profile of N_2 during stages 1 and 2 suggests the unsteady behavior of the following reaction:

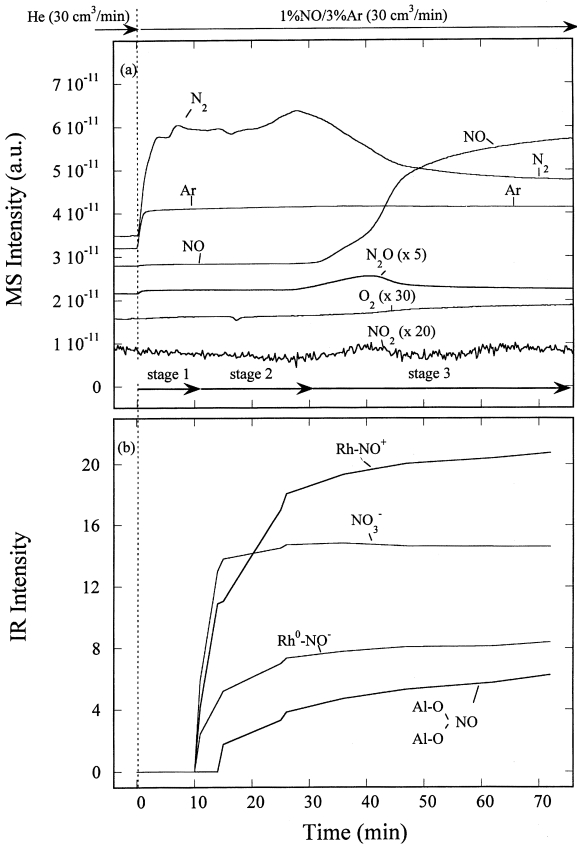

Fig. 1. (a) MS analysis of IR reactor effluent during the step switch from He (30 cm^3/min) to 1% NO (30 cm^3/min). (b) IR intensity of adsorbates vs. time, on $Rh/A1_2O_3$(125 mg) at 673 K.

$$2Rh + 2NO \rightarrow 2Rh - O + N_2 \quad (1)$$

Reaction (1) is a global reaction and its elementary steps will be discussed later.

During Stage 2, $Rh–NO^+$ at 1893 cm^{-1}, $Rh^0–NO^-$ at 1644 cm^{-1}, nitrate ion at 1361 cm^{-1} and bridging bidentate at 1540 cm^{-1} began to develop at 11 min as a result of modification of Rh surface by adsorbed oxygen, i.e. Rh–O. Rh–O slowly converts the reduced Rh sites to Rh^+ sites, which chemisorb NO as $Rh–NO^+$. Fig. 1(a) shows that as the $Rh–NO^+$ intensity approached 90% of its saturated level; gaseous NO emerged at Stage 3, indicating the loss of catalyst activity. The loss of NO decomposition activity allows populating of non-dissociated NO on the surface, such as $Rh^0–NO^-$ and $Rh–NO^+$. $Rh^0–NO^-$ and $Rh–NO^+$ may react with adsorbed N, already existing on the

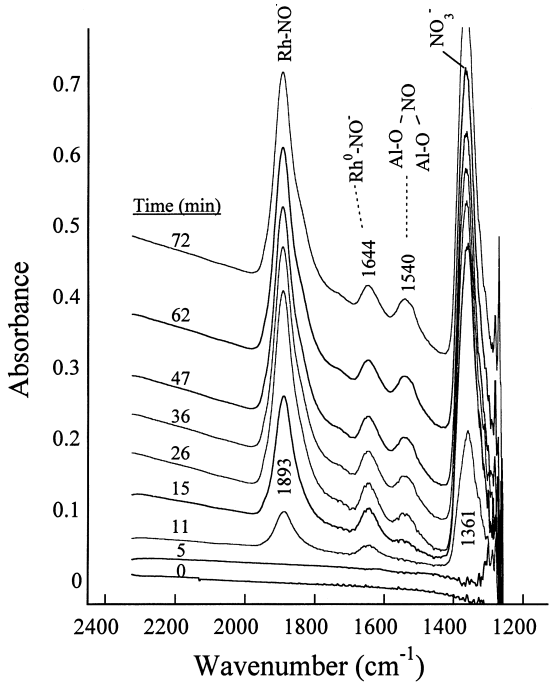

Fig. 2. IR spectra of adsorbates during the step switch from He (30 cm^3/min) to 1% NO (30 cm^3/min) on Rh/Al_2O_3 at 673 K.

surface, resulting in N_2O formation. The formation of N_2O from adsorbed N and NO is further supported by the crossover between the decrease in the N_2 profile and increase in the NO profile as shown in Fig. 1(a).

3.2. NO decomposition on Rh/C

Fig. 3(a) shows the MS analysis of the IR reactor-cell effluent during the 1% NO step switch reaction studies on Rh/C at 673 K. The IR spectra of the adsorbates corresponding to the MS profiles are shown in Fig. 4. The step switch from He to 1% NO resulted in 100% conversion of NO and the formation of N_2 during the first 50 min of the reaction. The step switch also caused the development of the adsorbates at 1400, 1277, 1151 and 1101 cm^{-1} and approached saturation at 20 min as shown in Fig. 3(b) and Fig. 4. The band at 1400 cm^{-1} has been assigned to oxygen species on carbon surface in the form of esters, phenols or carbonates [17,18]. The band at 1277 cm^{-1} could also be due to oxygen species on the surface, resulting from C–O stretches in species like aromatic ethers. The bands at 1151 and 1101 cm^{-1} were assigned to the C–N

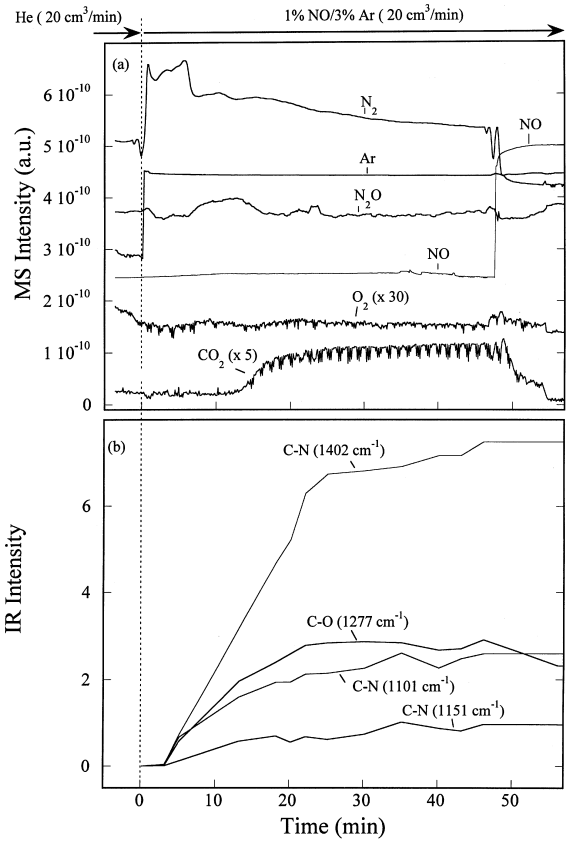

Fig. 3. (a) MS analysis of IR reactor effluent during the step switch from He (20 cm^3/min) to 1% NO (20 cm^3/min). (b) IR intensity of adsorbates vs. time, on Rh/C (100 mg) at 673 K.

species on the surface [19]. The assignment of these species was further verified by IR studies of O_2 and N_2 adsorption on carbon-supported catalysts surface [20].

Comparison of the results in Figs. 1 and 3 shows that the NO reaction on Rh/C differed from that on Rh/Al_2O_3 in the development and formation of both, the adsorbates and products. The major products on Rh/C are N_2 and CO_2. CO_2 emerged at the moment when the C–O species at 1402 cm^{-1} showed a drastic increase in its intensity. The result suggests that the C–O species is a precursor toward CO_2 formation.

3.3. NO decomposition on Pd/Al_2O_3

Fig. 5(a) shows the MS analysis of the IR reactor cell effluent during the 1% NO step switch reaction studies on Pd/Al_2O_3 at 673 K. The IR spectra of the ad-

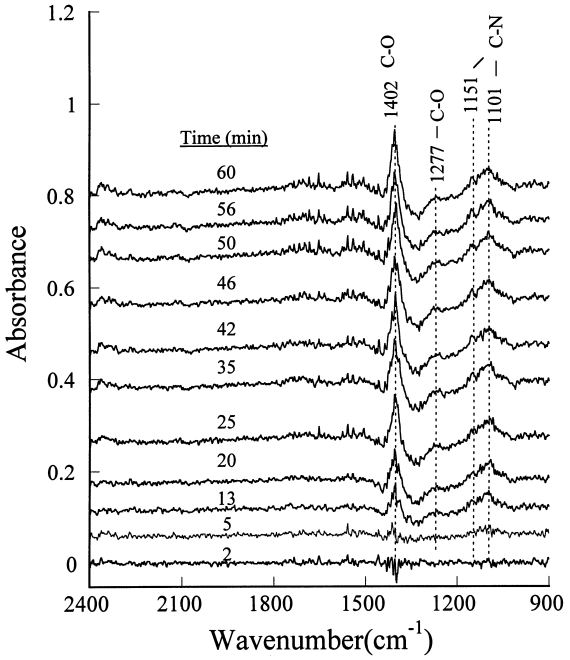

Fig. 4. IR spectra of adsorbates during the step switch from He (20 cm^3/min) to 1% NO (20 cm^3/min) on Rh/C at 673 K.

sorbates corresponding to the MS profiles are shown in Fig. 6. Like the reaction on Rh/Al_2O_3, the NO decomposition process on Pd/Al_2O_3 can be divided into three stages. Stage 1 is near-complete conversions of NO; Stage 2 is the NO adsorbate development; and Stage 3 is the emergence of NO and O_2. The major difference between Pd/Al_2O_3 and Rh/Al_2O_3 is that Pd/Al_2O_3 catalyzes the formation of significant amounts of O_2.

The development of Pd–NO^+ at 1802 cm^{-1} at 2.9 min in Stage 2 reflects an increase in the concentration of Pd^+ produced by adsorbed oxygen from NO dissociation. As the intensity of Pd–NO^+ reached a constant level, as shown in Fig. 5(b), gaseous NO and O_2 emerged while the reaction process moved to Stage 3.

3.4. NO decomposition on Pd/C

Fig. 7(a) shows the MS analysis of the reactor effluent during the 1% NO step switch reaction studies on Pd/C at 673 K. The IR spectra of the adsorbates corresponding to the MS profiles are shown in Fig. 8. The step switch to 1% NO resulted in near-100%

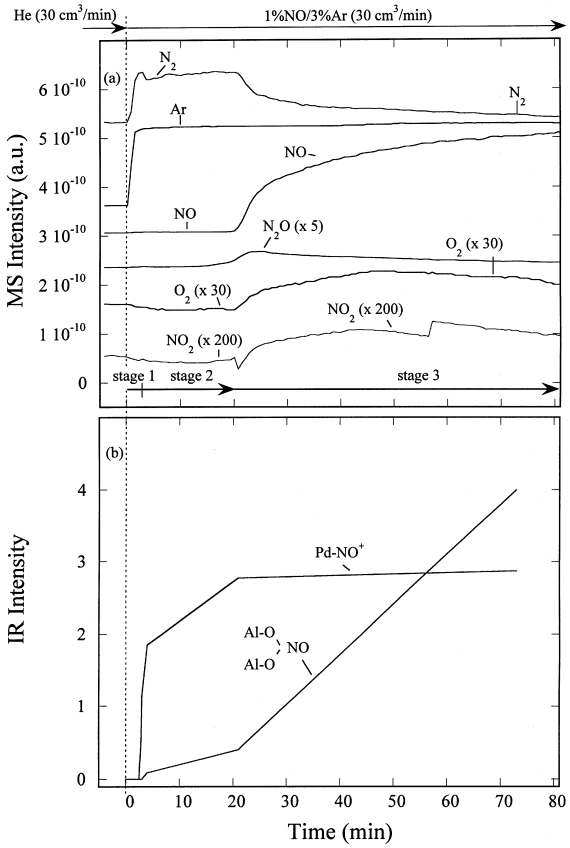

Fig. 5. (a) MS analysis of IR reactor effluent during the step switch from He (30 cm^3/min) to 1% NO (30 cm^3/min). (b) IR intensity of adsorbates vs. time, on Pd/Al_2O_3(125 mg) at 673 K.

conversions of NO and the formation on N_2, during 52 min of the reaction. The development of Pd–NO^+ at 1770 cm^{-1}, C=O at 1655 cm^{-1} [12,18], C–O at 1398 cm^{-1} and C–N at 1132 $cm^{-1}$was also observed. The appearance of Pd–NO^+ reflects an increase in the concentration of Pd^+ produced by adsorbed oxygen from NO dissociation. As in Pd/Al_2O_3, a significant amount of O_2 was produced with the emergence of gaseous NO. Comparison of the results of Rh/C in Fig. 3(a) and Pd/C in Fig. 7(a), reveals that Rh/C catalyzes the formation of CO_2, but Pd/C catalyzes the formation of O_2.

4. Discussion

Table 2 shows the activity and selectivity of the different catalysts for the NO decomposition. The amount

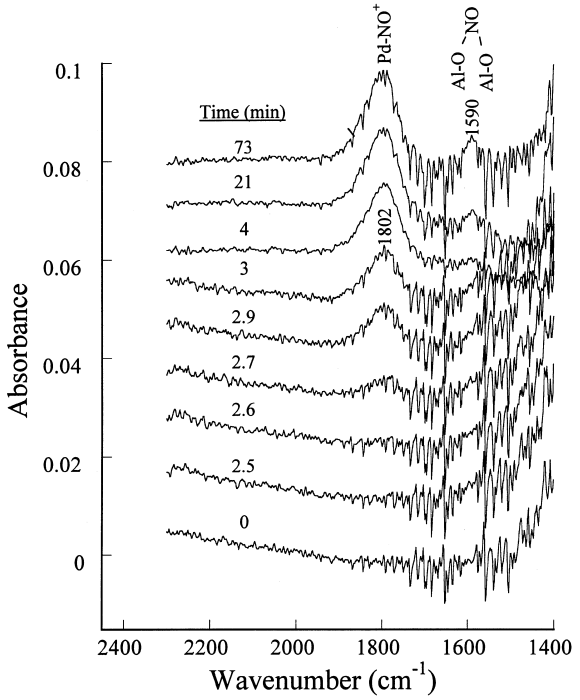

Fig. 6. IR spectra of adsorbates during the step switch from He (30 cm^3/min) to 1% NO (30 cm^3/min) on Pd/Al_2O_3 at 673 K.

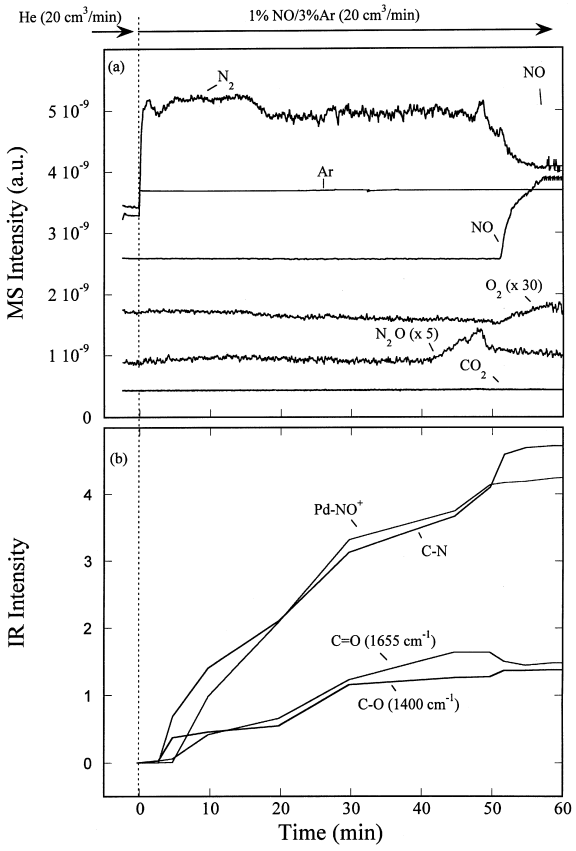

Fig. 7. (a) MS analysis of IR reactor effluent during the step switch from He (20 cm^3/min) to 1% NO (20 cm^3/min). (b) IR intensity of adsorbates vs. time, on Pd/C (100 mg) at 673 K.

of oxygen adsorbed from $2NO + 2S \rightarrow N_2 + 2O–S$ was normalized by catalyst weight. It can be inferred from Table 2 that the carbon-supported catalysts have the ability to uptake more oxygen than alumina-supported catalysts. Comparison of the amount of adsorbed oxygen with the number of metal surface atoms (Table 2) reveals that the oxygen adsorbed on the surface diffuses to the bulk causing the formation of bulk oxides.

The behavior of the catalyst (i.e. activity, selectivity and adsorbates on the catalyst surface) may be interpreted using the proposed mechanism listed in Table 3. Formation of different products can be explained by the structure of adsorbates and their reaction pathways on the catalyst surface. Prior to the emergence of gaseous NO (i.e. Stage 1), instantaneous dissociation of adsorbed NO (Step 2 in Table 3) takes place on both Pd^0 and Rh^0 surfaces of the Al_2O_3-supported catalysts. The facile nature of NO dissociation allows the immediate formation of N_2 (Step 3) and near-100% conversions of NO on the catalyst surface. Absence of steric crowding of adsorbed NO molecules on the catalyst surface is attributed to the facileness of Step 2. The instantaneous consumption of the precursor adsorbates for the NO dissociation yielded no adsorbate IR bands, preventing verification of the nature of the NO adsorbate in Step 2.

Our previous transient studies have revealed that Rh^0–NO^- at 1644 cm^{-1} and Pd^0–NO at 1745 cm^{-1} are the active adsorbates for NO dissociation to form adsorbed N and adsorbed O during the NO–CO reaction [21,22]. It is expected that the same adsorbates may decompose in the absence of CO and serve as the active adsorbates for NO decomposition. For the Rh/Al_2O_3 catalyst, Rh–NO^+ was not the active adsorbate for NO dissociation. As it approached the saturated level, Rh/Al_2O_3 began losing its activity for NO decomposition. The same trend was observed for Pd–NO^+ and NO conversion activity over Pd/Al_2O_3.

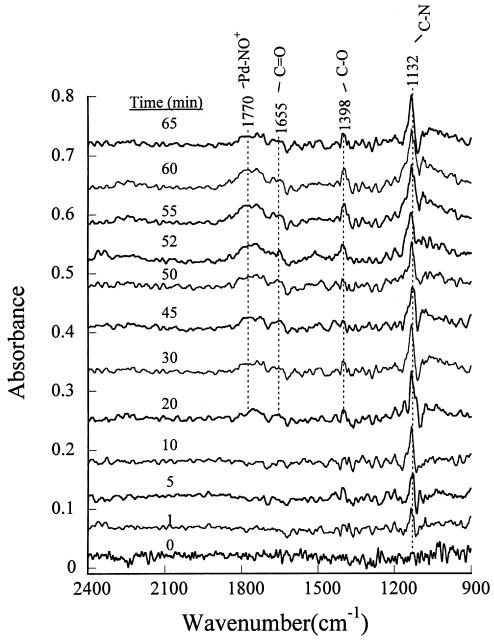

Fig. 8. IR spectra of adsorbates during the step switch from He (20 cm^3/min) to 1% NO (20 cm^3/min) on Pd/C at 673 K.

The formation of N_2O (Step 5) requires both, adsorbed N and adsorbed NO. Our previous studies have shown this step takes place on the reduced metal sites [21]. Although different amounts of N_2O were produced on these four catalysts, all the N_2O formation occurred near the crossover point, where the N_2 profile decreased and the NO profile increased. The results indicate that N_2O formed at the optimum concentration of adsorbed N and adsorbed NO.

The lack of oxygen formation (Step 6) during the 100% NO conversion (i.e. Stage 1 on these four catalysts) suggests that the NO conversion to N_2 at this stage is not a catalytic process; instead, it is a stoichiometric reaction as shown in reaction (1). A process is defined as catalytic when active sites are regenerated and the product formation is continuous. The absence of oxygen desorption during the high NO conversion is further evidenced by the absence of NO_2 formation (Step 7). It has been well established that NO_2 can be formed from either Step 7 or by the gas-phase reaction of NO with O_2. The observations of the present study agreed well with several studies, which have suggested that adsorbed O (i.e., S–O, where S is Rh or Pd) remains on the surface [10,23,24]. Unless the catalyst has the ability to desorb oxygen, S–O from reaction (1) will accumulate on the surface and blocks the sites for NO dissociation resulting in the increase in the surface coverage of the IR-observable species (active and spectator adsorbate).

Interestingly, each of these four different catalysts exhibits different abilities to manipulate adsorbed oxygen. Rh/Al_2O_3 shows the weakest oxygen desorption capability, letting most of oxygen to be accumulated on the Rh surface and losing NO decomposition activity. The Rh/C catalyst exhibits the ability of spilling over the adsorbed O from Rh surface onto the carbon support and reacting with carbon to produce CO_2 as in Step 8 (i.e. gasification of the carbon). Production of CO_2 in Fig. 3a appears to result from migration of adsorbed oxygen onto the carbon surface to form the C–O species at 1277 and 1402 cm^{-1} as seen in Fig. 4. Rh/C catalyst eventually lost its activity for CO_2 formation, indicating that Step 8 was interrupted. The loss of Rh/C activity for CO_2 formation is not surprising. As the carbon, located near the interface of Rh metal and carbon support, is being removed by CO_2

Table 2
Activity and selectivity of the catalysts for NO decomposition at 673 K

	Rh/Al_2O_3	Rh/C	Pd/Al_2O_3	Pd/C
Amount of oxygen adsorbed (μmol/g)[a]	1303	1759	912	1800
Number of metal surface atom (μmol/g)[b]	880.4	937.1	686.5	636.8
W/F (g/cm^3 s)	0.25	0.3	0.29	0.3
Steady-state conversion after breakthrough (%)	14.0	100[c]	20.29	21.59
Yield of O_2 (%)[d]	0.4	0.0	1.74	1.4
Yield of CO_2 (%)	0.0	22.6	0.0	0.0

[a] During stages 1 and 2, and normalized for g basis.
[b] Calculated from XRD data.
[c] Conversion during steady-state formation of CO_2.
[d] Amount of O_2 produced/amount of NO in the reactant stream.

Table 3
Proposed mechanism for NO decomposition

Reaction steps		Rh/Al_2O_3	Pd/Al_2O_3	Rh/C	Pd/C
Step 1	$S^{0a} + NO \leftrightarrow S^0 - NO^-$	+[b]	+	+	+
Step 2	S^0–$NO^- + S^0 \rightarrow S–N + S–O\ (S^+)$	+	+	+	+
Step 3	$S–N + S–N \rightarrow 2S + N_2$	+	+	+	+
Step 4	$S^+ + NO \leftrightarrow S^+$–NO	+	+	−[c]	+
Step 5	$S–NO + S–N \rightarrow 2S + N_2O$	+	+	+	+
Step 6	$S–O + S–O \leftrightarrow 2S + O_2$	+	+	−	+
Step 7	$S–NO + S–O \rightarrow 2S + NO_2$	+	+	−	−
Step 8	$S–O + C \rightarrow S + C + CO_2$	−	−	+	−

[a] S is Rh^0 or Pd^0 site.
[b] Indicates occurrence of the step.
[c] Indicates absence of the step.

formation, the Rh metal and carbon surface are expected to undergo dramatic modifications causing either decreasing Rh–C interface or losing the contact between Rh and carbon. SEM studies have shown that NO reaction with carbon causes pitting [15].

Absence of Step 8, CO_2 formation, on Pd/C is in good agreement with the literature observations [25]. Pd shows the ability to desorb oxygen after saturation is reached as observed in Pd/Al_2O_3 and Pd/C. The difference in the activity of the Rh/C and Pd/C catalysts towards desorption of oxygen could be due to the difference in the binding energy of oxygen and Rh (145 kcal/mol), and Pd (87 kcal/mol) [26,27]. Thus, it may be easier for adsorbed oxygen on Pd to recombine for desorption as molecular oxygen. The difference in Pd/C and Pd/Al_2O_3 in oxygen desorption could be due to dispersion of metal particles (Table 2) or metal–support interaction. Lack of detailed structural surface information does not allow elucidation of the role of metal–support interaction in the oxygen desorption.

As discussed earlier, the difference in the activity and selectivity of these four catalysts for the NO decomposition and reaction can be attributed to the difference in their capability to activate each elementary step listed in Table 3. The facile nature of NO dissociation (Step 2) and N_2 formation (Step 3) points to steps 6 and 8 as the rate-limiting steps for the overall reaction. Rh promotes Step 8 for CO_2 formation while Pd activates Step 6 for O_2 formation on the carbon-based catalysts. The rates of these steps, which are temperature-dependent, are clearly not fast enough compared to NO dissociation (Step 2) resulting in the accumulation of adsorbed oxygen and then loss of the catalyst activity. We have also studied the reaction on Rh/Al_2O_3 and Pd/Al_2O_3 at 573 K. Decreasing the temperature from 673 to 573 K resulted in shortening the time for near-100% NO conversion (i.e. Stage 1) for Rh/Al_2O_3 from 31 to 19 min and for Pd/Al_2O_3 from 20 to 14 min. Increasing the reaction temperature on Rh/C and Pd/C to 773 K resulted in extending the activity for near-100% conversion for Rh/C from 51 to 4 h and for Pd/C from 52 to 75 min. These differences could be attributed to the dependence of steps 6 and 8 on temperature, where high-temperature facilitates the removal of surface (i.e. adsorbed) oxygen.

5. Conclusions

The results of this study can be summarized as follows:

1. NO decomposition on Rh/Al_2O_3 produced N_2 initially. As oxygen on the surface accumulated, Rh–NO^+ at 1893 cm^{-1}, Rh–NO^- at 1644 cm^{-1} developed, and the catalyst lost NO decomposition activity.
2. NO decomposition on Rh/C produced N_2 and CO_2. The adsorbed oxygen on the metal migrated to the support, resulting in the development of C–O stretches at 1402 cm^{-1}, which served as the precursor adsorbate for CO_2 formation.
3. NO decomposition on Pd/Al_2O_3 produced N_2 initially. As oxygen on the surface accumulated, Pd–NO^+ at 1802 cm^{-1} developed. Further ac-

cumulation of adsorbed oxygen caused oxygen desorption and partial loss of the catalyst activity.
4. Use of carbon as a support for Pd promotes O_2 desorption. Adsorbed N and O on carbon does not appear to participate in product formation.

The differences in the ability of the catalyst for manipulation of adsorbed oxygen resulting in different NO decomposition activities.

Acknowledgements

The authors gratefully acknowledge financial support for this research from the U.S. Department of Energy, Grant DE-FG22-95PC955224.

References

[1] M. Iwamoto, Future opportunities in Catalytic and Separation Technology, Studies in Surface Science and Catalysis, Elsevier, Amsterdam, 1990.
[2] K.C. Taylor, Catal. Rev.-Sci. Eng. 35 (1993) 457.
[3] R.M. Heck, R.J. Farrauto, Catalytic Air Pollution Control, Commercial Technology, Van Nostrand Reinhold, 1995.
[4] R. Krishnamurthy, S.S.C. Chuang, M.W. Balakos, J. Catal. 157 (1995) 512.
[5] B.J. Ku, J.K. Lee, D. Park, H. Rhee, Ind. Eng. Chem. Res. 33 (1994) 2868.
[6] M. Shelef, Catal. Rev.-Sci. Eng. 95 (1995) 209.
[7] J.W. Hightower, D.A. Van Leirsburg, In: R.L. Klimisch, J.G. Larson (Eds.), The Catalytic Chemistry of Nitrogen Oxides, Plenum Press, New York, 1975, p. 63.
[8] Y. Li, W.K. Hall, J. Catal. 129 (1991) 202.
[9] A.W. Aylor, S.C. Reimer, J.A. Larsen, A.T. Bell, J. Catal. 157 (1995) 592.
[10] S.S.C. Chuang, C-D. Tan, J. Phys. Chem. B 101 (1997) 3000.
[11] P.M. Eisenberger (Ed.), Report on Basic Research Needs for Vehicles of the Future, Princeton Materials Institute, Princeton University, 1995.
[12] E. Suuberg, H. Teng, J. Calo, Energy Fuels 6 (1992) 398.
[13] M.J. Illan-Gomez, A. Linares-Solano, L.R. Radovic, C. Salinas-Martinez de Lecea, Energy Fuels 10 (1996) 158.
[14] E. Ruckenstein, Y.H. Hu, Ind. Eng. Chem. Res. 36 (1997) 2533.
[15] T. Inui, T. Otowa, Y. Takegami, Ind. Eng. Chem. Prod. Res. Dev. 21 (1982) 56.
[16] S.S. C Chuang, M.A. Brundage, M.W. Balakos, G. Srinivas, Appl. Spectrosc. 49 (1995) 1151.
[17] C.H. Rochester, B.J. Meldrum, J. Chem. Soc., Faraday Trans. 86 (1990) 3647.C.H.
[18] M.A. Vannice, R.T.K. Baker, A. Dandekar, Carbon, 1998, submitted for publication.
[19] C.H. Rochester, B.J. Meldrum, J. Chem. Soc., Faraday Trans. 86 (1990) 1881.
[20] R. Krishnamurthy, M.S. Thesis, The University of Akron, 1998.
[21] R. Krishnamurthy, S.S.C. Chuang, J. Phys. Chem. 99 (1995) 16727.
[22] K. Almusaiteer, S.S.C. Chuang, J. Catal. 180 (1998) 161.
[23] S.H. Oh, J.E. Carpenter, J. Catal. 101 (1986) 114.
[24] R.D. Ramsier, Q. Gao, H.N. Walteburg, K.W. Lee, O.W. Nooij, L. Lefferts, J.T. Yates Jr., Surf. Sci. 320 (1994) 209.
[25] M.A. Salas-Peregrin, M. Primet, H. Praliaud, Appl. Catal. B 8 (1996) 79.
[26] A.T. Bell, in: E. Shustorovich (Ed.), Metal-Surface Reaction Energetics: Theory and Applications to Heterogeneous Catalysis, Chemisorption, and Surface Diffusion, VCH, USA, 1991, Chapter 5, p. 191.
[27] A. de Koster, R.A. van Santen, J. Vac. Sci. Technol. A 6 (1988) 1128.